IEEE Photonics Journal
An IEEE Photonics Society Publication

Open Access

A Convergent Wireline and Wireless Time-and-Wavelength-Division-Multiplexed Passive Optical Network

Volume 7, Number 3, June 2015

C. W. Chow, Senior Member, IEEE
J. Y. Sung
C. H. Yeh

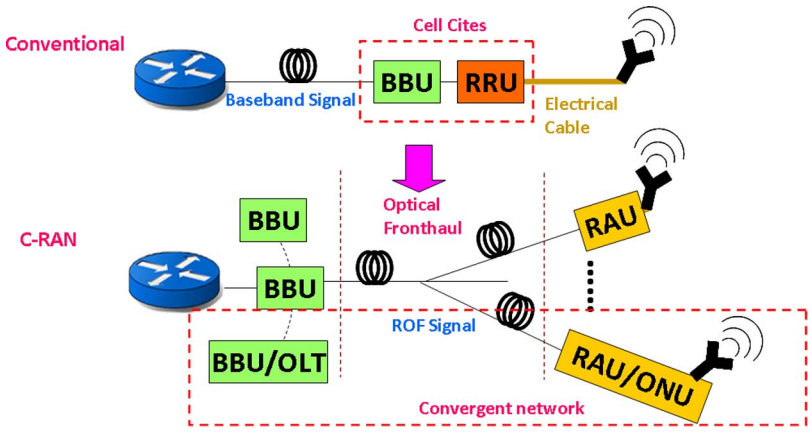

DOI: 10.1109/JPHOT.2015.2440339
1943-0655

IEEE photonics SOCIETY

IEEE

A Convergent Wireline and Wireless Time-and-Wavelength-Division-Multiplexed Passive Optical Network

C. W. Chow,[1] *Senior Member, IEEE*, J. Y. Sung,[1] and C. H. Yeh[2]

[1]Department of Photonics and Institute of Electro-Optical Engineering, National Chiao Tung University, Hsinchu 30010, Taiwan
[2]Department of Photonics, Feng Chia University, Taichung 40724, Taiwan

DOI: 10.1109/JPHOT.2015.2440339

Manuscript received May 10, 2015; revised May 27, 2015; accepted May 28, 2015. Date of current version June 15, 2015. This work was supported in part by the Ministry of Science and Technology, Taiwan, under Contract MOST-103-2221-E-009-030-MY3 and Contract MOST-103-2218-E-035-011-MY3; by the Aim for the Top University Plan, Taiwan; and by the Ministry of Education, Taiwan. Corresponding author: C. W. Chow (e-mail: cwchow@faculty.nctu.edu.tw).

Abstract: We propose and demonstrate a convergent wireline and wireless access network using time-and-wavelength-division-multiplexed passive optical network (TWDM-PON) architecture. Bidirectional 40-km single-mode-fiber transmissions (including the 60-GHz wireless transmission) satisfying the forward error correction limit are demonstrated, with data rates of ~10 Gb/s per wavelength in the downstream signal and 17.50 Gb/s per wavelength in the upstream signal. To achieve higher data rate, bit-loading orthogonal frequency-division modulation was used. We also analyze the laser-linewidth-induced performance variation to the signal generated by optical beating and the baseband signal.

Index Terms: Optical communications, wavelength-division-multiplex passive optical network (WDM-PON), convergent wireline and wireless network.

1. Introduction

We have observed a significant increase in bandwidth demands of mobile communications for the past few years. People want to access to the network anywhere and anytime. In the near future, there will be much more wireless IP traffic than wireline traffic [1]. That is why many researchers and operators are looking for novel solutions for next generation wireless communications. This trend also agrees with the Edholm's Law of Bandwidth [2], predicting that the data rates of wireline and wireless will converge eventually. This means that in the future, a unified (or convergent) optical wireline and wireless network is required for providing both fixed and mobile services to users [3]–[8]. Besides, millimeter-wave (mm-wave) frequency bands [3], [4] are considered for future wireless transmission. On the other hand, wireline networks are continuously evolving to meet the Internet bandwidth demand. Recently, the second-stage of next generation PON (NG-PON2) has been standardized. According to the NG-PON2 recommendation, time and wavelength division-multiplexed (TWDM) PON [9]–[12] has been selected as the primary architecture for NG-PON2. In the TWDM-PON architecture, the existing optical distribution network (ODN) can be re-used. In the optical line terminal (OLT), four sets of transmitters (Tx) and receivers (Rx) are stacked to increase the aggregated data rate of the downstream data. At the user's side optical networking unit (ONU), an optical tunable filter (OTF) is needed to

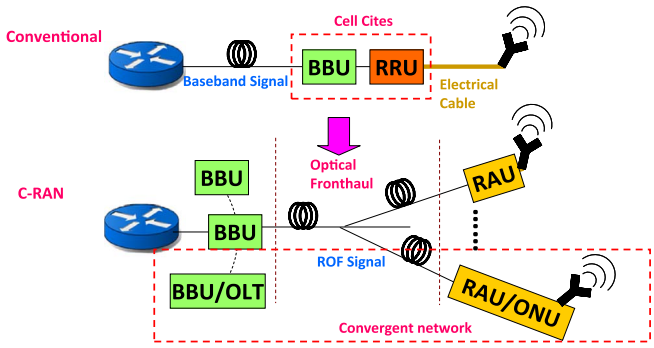

Fig. 1. Architectures of conventional macrocell wireless system and the emerging C-RAN. BBU: baseband processing unit; RAU: remote antenna unit; OLT: optical line terminal; ONU: optical networking unit.

select the downstream wavelength, and tunable Tx is used to generate the upstream signal. Hence, a convergent optical network supporting both future wireline and wireless communications, using the TWDM-PON ODN is important for near future.

In this work, we propose and demonstrate a convergent wireline and wireless access network using TWDM-PON architecture. Bi-directional 40 km single-mode-fiber (SMF) transmissions satisfying the forward-error-correction (FEC) limit are demonstrated. We use orthogonal frequency division multiplexing (OFDM) modulation formats to carry both downstream and upstream data, since OFDM is highly spectral-efficient and highly tolerant to fiber chromatic dispersion [13], [14]. Besides, the OFDM subcarriers can be aggregated and de-aggregated electrically and providing both wireline and wireless applications using different subcarriers. Hence, OFDM is considered as one of the promising modulation formats for next generation PON [13]. Besides, we also analyze the laser-linewidth induced performance variation to the signal generated by optical beating and the baseband signal.

2. Principle of Optical Fronthaul and Proposed Convergent Network

Next-generation wireless communications will use high-frequency bands to avoid the overcrowded low-frequency bands. However, due to the relatively high atmospheric attenuation in the mm-wave frequency bands, the wireless transmission distance (wireless cell size) will greatly reduce. This means much more cell sites are needed to provide the same coverage. Because of this, the expensive cell site should be cost-down to simple remote antenna unit (RAU). At the same time, the baseband processing unit (BBU), which is traditionally located at the cell site, will be moved towards the core network. The original remote radio unit (RRU) will be simplified to RAU by shifting most of the signal processing functions to the BBU. Hence only optical-to-electrical (OE) and electrical-to-optical (EO) conversions and antenna are left in the RAU. So that the expensive BBUs can be connected together for resource sharing in the core-network; while each BBU can connect many RAUs using radio-over-fiber (ROF) technique via the optical fiber network (also know as optical fronthaul). Fig. 1 illustrates the above system concept. The cell sites are simplified to RAU, and the radio frequency (RF) signals are directly transmitted from the BBU to the RAU via optical fiber network using ROF. The above mentioned concept is also known as cloud-based radio access network (C-RAN) [4]. We also believe that this optical fronthaul can be integrated with the future PON system, such as the TWDM-PON. As also shown in Fig. 1, the BBU can combine with the PON OLT while the RAU can combine with the ONU; hence a convergent wireline and wireless network architecture can be formed. This architecture can reduce the cost and power consumption since the expensive BBU/OLT can be shared among operators using the core network, whereas the RAU/ONU can be significantly simplified and cheaper.

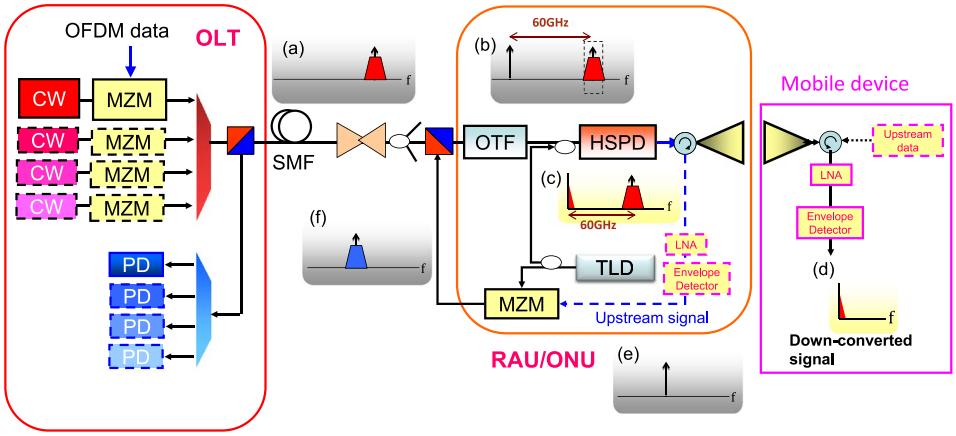

Fig. 2. Architecture of the proposed convergent wireline and wireless access network. OLT: optical line terminal; MZM: Mach-Zehnder modulator; SMF: single mode fiber; OTF: optical tunable filter; HSPD: high speed photodiode; TLD: tunable laser diode; LNA: low noise amplifier; RAU: remote antenna unit; ONU: optical networking unit. (Insets) Schematic optical and electrical spectra.

3. Proof-of-Concept Experimental Demonstration

The proof-of-concept convergent wireline and wireless access network using TWDM-PON architecture is shown in Fig. 2. The insets show the corresponding schematic optical or electrical spectra at different locations. A continuous-wave (CW) signal is launched to a Mach-Zehnder modulator (MZM), which is connect to an arbitrary waveform generator to produce the OFDM downstream signal [the schematic optical spectrum shown in Fig. 2(a)]. OFDM generation uses off-line Matlab program, including serial-to-parallel conversion, quadrature amplitude modulation (QAM) symbol encoding, and IFFT and cyclic prefix (CP) insertion. The OFDM signal has FFT size of 512 and the CP size is 1/32. The arbitrary waveform generator has 3.2 GHz bandwidth and 8 GSample/s sampling rate. The sampling rate of 8 GSample/s used in the experiment is limited by the maximum sampling rate of our AWG (Tektronix AWG7082C). Then, the four different wavelength all-optical OFDM downstream signals can be combined and transmitted to the RAU/ONU through 40 km SMF, an erbium-doped fiber amplifier (EDFA) and optical splitters. At the RAU/ONU, an optical tunable filter (OTF) selects one channel of the OFDM signal, which is then launch to the high speed photodiode (HSPD) (a PIN PD from u2t photonics is used, the 3-dB frequency response is 75 GHz, responsivity is 0.65 A/W, polarization dependent loss is 0.2 dB, optical return loss is 31.8 dB and dark current is 6 nA) together with a CW signal produced by a local tunable laser diode (TLD). The OTF used in this proof-of-concept demonstration is a thin-film filter; however, integrated silicon-based optical filter can be used to lower the cost of the RAU/ONU [15]. The schematic optical spectrum is shown in Fig. 2(b). The beating of the local CW and the downstream OFDM at the HSPD produces the upconverted RF signal, as shown in Fig. 2(c). The mm-wave signal after the HSPD is first amplified by a RF amplifier (65 GHz bandwidth and small signal gain of 10 dB from SHF Comm. Tech.), and then emitted and received via a pair of v-band horn antenna (pyramidal shaped using waveguide WR-15 from Quinstar). After the wireless transmission, at the mobile device the signal is received, amplified by a low noise amplifier (LNA) (30 dB gain, noise-figure 4.5 dB from Quinstar), and envelope-detected [see Fig. 2(d)] for the bit-error-rate (BER) measurement. The envelope-detector is from Quinstar QEA broadband detector. It operates at V-band (50–75 GHz), with minimum sensitivity of 800 mV/mW, maximum input power of 100 mW. The envelope-detector provides an output voltage which is directly proportional to the power level of the received wireless RF signal without needing any external DC bias. Hence, it is useful for down-converting the wireless signal to baseband data. Here, the wireless transmission distance is about 10 cm. Much higher wireless transmission is expected if high power RF amplifier is available after the HSPD to amplify the signal for wireless transmission.

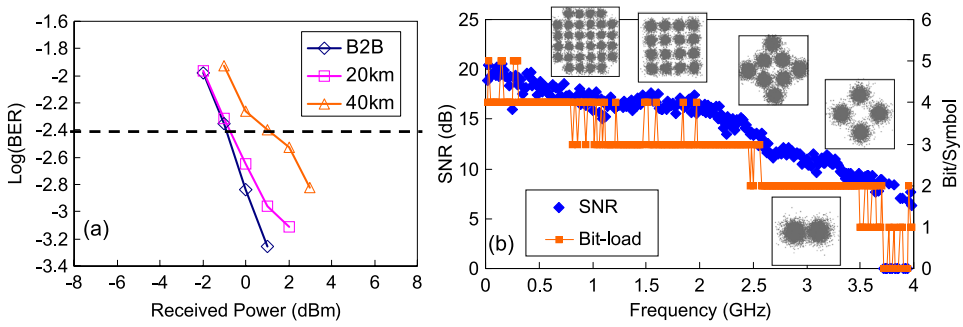

Fig. 3. (a) Measured BER of the downstream OFDM signal with SMF and 60 GHz wireless transmissions. (b) Measured SNR performance and bits/symbol.

For the upstream signal generation, the CW signal from the same TLD source at the RAU/ONU is used. The CW signal is launched to a MZM at the RAU/ONU to produce the upstream signal of the network [see Fig. 2(e) and (f)]. The upstream signal is then sent back and received by a PIN PD at the OLT. The proposed architecture not only supports the TWDM-PON architecture, but also provides flexible adjustment of wireless transmission frequencies achieved by fine tuning of the TLD wavelength. In the experiment, the separation between the CW and wireless downstream is set at 60 GHz. However, the wavelength of the CW can be adjusted to produce different mm-wave frequencies for frequency reuse in the wireless cell. Besides, if the wavelength needed of the TLD to produce the downstream wireless signal and the wavelength needed to produce the upstream signal are different, the TLD wavelength can be adjusted to emit at different time-slots.

4. Results

We first measure the downstream signal. As shown in Fig. 2, the optical OFDM signal after passing through 40 km SMF is combined with the CW signal with wavelength separation of 60 GHz generated by a local TLD at the RAU/ONU via a 3-dB fiber coupler. The beating of the local CW and the downstream OFDM at the HSPD produces the upconverted mm-wave signal, which is then emitted and received via a pair of horn antenna. At the mobile device, a wireless signal is received, amplified, and envelope-detected. Then the detected signal is captured by a real-time oscilloscope for demodulation. The OFDM demodulation process includes off-line synchronization, FFT, one-tap equalization, CP removal and QAM symbol decoding. As different downstream OFDM subcarriers can be assigned for different applications; hence at the ONU, the baseband downstream OFDM can be received without emitting our wirelessly at some time-slot, and some OFDM subcarrier can be de-aggregated electronically for the ONU wireline applications.

Fig. 3(a) shows the measured BER performance of the downstream OFDM signal after 20 km or 40 km SMF and 60 GHz wireless mm-wave transmission. To achieve higher data rate, bit-loading technique is used for the OFDM signal. The level of bit-loading is determined by the signal-to-noise ratio (SNR). The data rate achieved is 9.82 Gb/s per wavelength (after the CP removal). The 4 GHz bandwidth is limited by the AWG. As the future TWDM-PON using 10 GHz optical transceiver per wavelength at the OLT, $\sim$25 Gb/s data rate (9.82 Gb/s $\times$ 2.5) per wavelength can be expected. Hence, a total capacity of $\sim$100 Gb/s can be achieved in the TWDM-PON system. The SNR and bits/symbol after 40 km SMF and 60 GHz wireless mm-wave transmission can be observed in Fig. 3(b). To achieve higher data rate, bit-loading is used. For higher SNR frequency band, 5 bits/symbol is used. The downstream measurements satisfy the FEC limit.

Fig. 4(a) shows the measured BER performance of the upstream OFDM signal after 20 km or 40 km SMF. The data rate achieved is 17.50 Gb/s in the upstream (after the CP removal). The upstream signal is in typical OFDM format encoded by the MZM at the RAU/ONU. As the bandwidth is about 4 GHz and enough CP is used, there is almost no power penalty, as shown in Fig. 4(a).

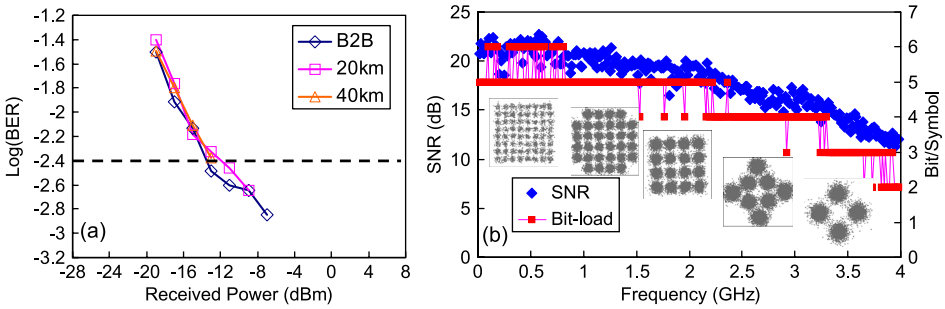

Fig. 4. (a) Measured BER of the upstream OFDM signal with SMF. (b) Measured SNR performance and bits/symbol.

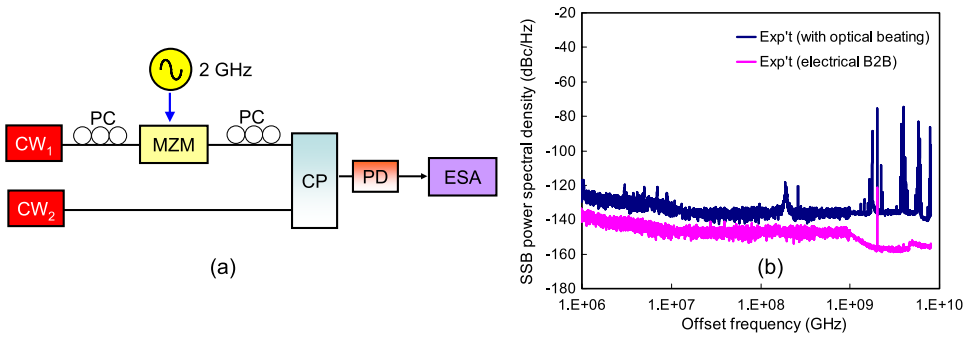

Fig. 5. (a) Experiment of direct beating of two independent lasers. (b) Measured SSB PSD.

As mentioned before, if higher bandwidth AWG is available, ~43.8 Gb/s (17.5 Gb/s × 2.5) can be expected for the upstream signal if 10 GHz optical transceiver is used at the ONU. The SNR and bits/symbol after 40 km SMF can be observed in Fig. 4(b). The upstream measurements also satisfy the FEC limit. The optical output power of the downstream OFDM signal per wavelength is 7 dBm. As shown in Fig. 3(a), the received optical power at the RAU to generate the FEC satisfied mm-wave signal is 2 dBm. By considering the insertion losses of the SMF, the 2 RBFs and the OTF are 0.2 dB/km, 1 dB and 3 dB respectively; and an EDFA of 28 dB gain (booster EDFA from GIP Tech.) is used, a split-ratio of 128 can be supported. This can satisfy the split-ratio of 64. The relatively poor receiver sensitivity for the downstream is due to the limited response of the PIN-PD used. Higher split-ratio can be expected if higher responsivity PD is available. We can observe that the upstream OFDM signal performance shown in Fig. 4(b) is better than the downstream wirelessly transmitted OFDM signal performance shown in Fig. 3(b). The reasons are due to the SNR degradation in the conversions from wireless to baseband signal and the beating laser linewidth. The analysis of laser-linewidth induced performance variation to the signal generated by optical beating and the baseband signal is discussed in the next section.

5. Analysis of Laser Linewidth Induced Degradation

We analyze the laser-linewidth induced performance variation to the signal generated by optical beating and the baseband signal. Fig. 5(a) shows the experimental setup used to emulate the generation of wireless RF signal by optical beating of two lasers. Although in the experiment (see Fig. 2), the wavelength separation of the two lasers are 0.48 nm (~60 GHz), in order to fit the measurement bandwidth of the electrical spectrum analyzer (ESA, Agilent E4440A), the wavelength separation in Fig. 5(a) is 0.08 nm (i.e. ~10 GHz). The setup in Fig. 5(a) consists of the two CW lasers, two polarization controllers (PCs), a 3-dB optical couplers (CP), a PD and an ESA. CW_1 is modulated by a 2 GHz sinusoidal signal and CW_2 is unmodulated. Fig. 5(b) shows the measured single-sideband (SSB) power spectral density (PSD) at the carrier frequency of

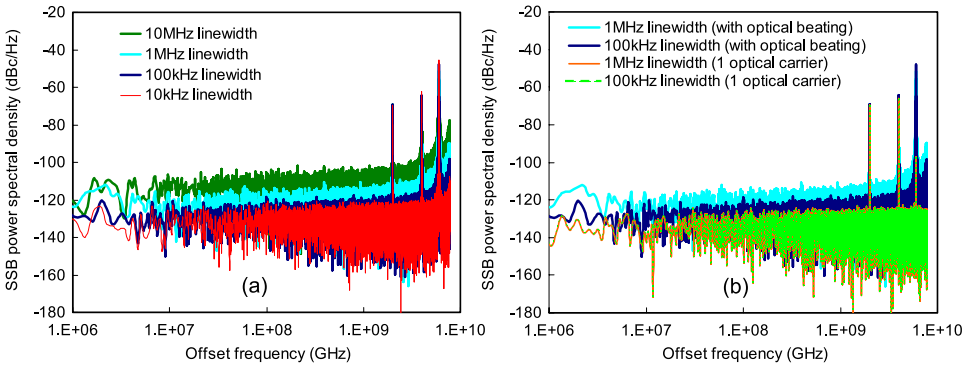

Fig. 6. Simulated SSB PSD of (a) direct beating of two independent lasers with different laser linewidths. (b) One single optical carrier.

2 GHz. During the 2 GHz sinusoidal modulation of the CW_1 signal, ±2 GHz and harmonics of ±4, ±6, and ±8 GHz are observed in the optical spectrum. This signal then beats with the CW_2 at the PD producing electrical tones at 4, 6, and 8 GHz shown in the RF spectrum. Some spurious peaks shown in Fig. 5(b) could result from fiber induced Fabry–Perot effect [16]–[18].

We numerically analyze the influence of laser linewidth induced performance variation using VPI Transmission Maker V7.5. The simulation setup is the same as Fig. 5(a). Fig. 6(a) shows the simulated SSB PSD using laser linewidths from 10 kHz to 10 MHz at carrier frequency of 2 GHz. We can observe that the noise floor increases when the laser linewidth increases. The noise floors in GHz frequency band are around −120, −110, and −100 dBc/Hz when the laser linewidths are 100 kHz, 1 MHz and 10 MHz respectively. Similar harmonic tones appeared in the simulation spectrum also agrees with the experimental spectrum. Then, CW_2 is turned-off, and the SSB PSD at carrier frequency of 2 GHz is measured, as shown in Fig. 6(b). We can observe that the noise floor is much lower. For example, if 100 kHz laser linewidth is used, the noise floor in GHz band is −120 dBc/Hz in the direct optical beating signal, while the noise floor is −130 dBc/Hz in a single optical carrier signal. This can provide one reason for the better performance of the upstream signal as shown in Fig. 4(b) when compared with the wirelessly transmitted downstream signal as shown in Fig. 3(b). Besides, we can also observe that when using signal optical carrier signal, the noise floors are nearly the same for different laser linewidths (100 kHz and 1 MHz), as also shown in Fig. 6(b). Hence the baseband signal transmission performance is independent of the laser linewidth.

6. Conclusion

In this work, we proposed and demonstrated a convergent wireline and wireless access network using TWDM-PON architecture. Bi-directional 40 km SMF transmissions (including the 60 GHz wireless transmission in the downstream) were demonstrated, with a data rates of ∼10 Gb/s per wavelength in the downstream signal and 17.50 Gb/s per wavelength in upstream signal. We also analyzed the laser-linewidth induced performance variation to the signal generated by optical beating and the baseband signal.

References

[1] *Cisco VNI Forecast*, 2014.
[2] S. Cherry, "Edholm's law of bandwidth," *IEEE Spectr.*, vol. 41, no. 7, pp. 58–60, Jul. 2004.
[3] G. K. Chang *et al.,* "Key technologies of WDM-PON for future converged optical broadband access networks," *J. Opt. Commun. Netw.*, vol. 1, no. 4, pp. C35–C50, Sep. 2009.
[4] C. Liu, J. Wang, L. Cheng, M. Zhu, and G. K. Chang, "Key microwave-photonics technologies for next-generation cloud-based radio access networks," *J. Lightw. Technol.*, vol. 32, no. 20, pp. 3452–3460, Oct. 2014.
[5] H. H. Lu *et al.,* "Bidirectional hybrid CATV/radio-over-fiber WDM transport system," *Opt. Lett.*, vol. 35, no. 3, pp. 279–282, Feb. 2010.

[6] P. C. Peng *et al.,* "DSBCS modulation scheme for hybrid wireless and cable television system," *Opt. Exp.*, vol. 22, no. 1, pp. 1135–1142, Jan. 2014.
[7] J. Y. Sung, K. T. Cheng, C. W. Chow, C. H. Yeh, and C. L. Pan, "A scalable and continuous-upgradable optical wireless and wired convergent access network," *Opt. Exp.*, vol. 22, no. 11, pp. 12 779–12 784, Jun. 2014.
[8] C. W. Chow and Y. H. Lin, "Convergent optical wired and wireless long-reach access network using high spectral-efficient modulation," *Opt. Exp.*, vol. 20, no. 8, pp. 9243–9248, Apr. 2012.
[9] Y. Ma *et al.,* "Demonstration of a 40Gb/s time and wavelength division multiplexed passive optical network prototype system," in *Proc. OFC*, 2012, pp. 1–3.
[10] Z. Li *et al.,* "Experimental demonstration of a symmetric 40-Gb/s TWDM-PON," in *Proc. OFC*, 2013, pp. 1–3.
[11] M. Bi *et al.,* "Simultaneous DPSK demodulation and chirp management using delay interferometer in symmetric 40-Gb/s capability TWDM-PON system," *Opt. Exp.*, vol. 21, no. 14, pp. 16 528–16 535, Jul. 2013.
[12] C. W. Chow, C. H. Yeh, K. Xu, J. Y. Sung, and H. K. Tsang, "TWDM-PON with signal remodulation and Rayleigh noise circumvention for NG-PON2," *IEEE Photon. J.*, vol. 5, no. 6, Dec. 2013, Art. ID. 7902306.
[13] N. Cvijetic, "OFDM in optical access networks," in *Proc. OFC*, 2011, pp. 384–398.
[14] C. W. Chow *et al.,* "Studies of OFDM signal for broadband optical access networks," *IEEE J. Sel. Areas Commun.*, vol. 28, no. 6, pp. 800–807, Aug. 2010.
[15] K. Xu *et al.,* "Demodulation of 20 Gbaud/s differential quadrature phase-shift keying signals using wavelength-tunable silicon microring resonators," *Opt. Lett.*, vol. 37, no. 16, pp. 3462–3464, Aug. 2012.
[16] J. Lasri, P. Devgan, R. Tang, and P. Kumar, "Self-starting optoelectronic oscillator for generating ultra-low-jitter high-rate (10 GHz or higher) optical pulses," *Opt. Exp.*, vol. 11, no. 12, pp. 1430–1435, 2003.
[17] H. Hasegawa, Y. Oikawa, and M. Nakazawa, "A 10-GHz optoelectronic oscillator at 850 nm using a single-mode VCSEL and a photonic crystal fiber," *IEEE Photon. Technol. Lett.*, vol. 19, no. 19, pp. 1451–1453, Oct. 2007.
[18] Y. C. Chi and G. R. Lin, "A-factor enhanced optoelectronic oscillator for 40-Gbit/s pulsed RZ-OOK transmission," *IEEE Trans. Micro. Theory Tech.*, vol. 62, no. 12, pp. 3216–3223, Dec. 2014.